

Forced extension of P-selectin construct using steered molecular dynamics

LÜ Shouqin & LONG Mian

National Microgravity Laboratory, Institute of Mechanics, Chinese Academy of Sciences, Beijing 100080, China
Correspondence should be addressed to Long Mian (e-mail: mlong@imech.ac.cn)

Abstract P-selectin, a 70-nm-long cellular adhesive molecule, possesses elastic and extensible properties when neutrophils roll over the activated endothelium of blood vessel in inflammatory reaction. Transient formation and dissociation of P-selectin/ligand bond on applied force of blood flow induces the extension of P-selectin and relevant ligands. Steered molecular dynamics simulations were performed to stretch a single P-selectin construct consisting of a lectin (Lec) domain and an epithelial growth factor (EGF)-like domain, where P-selectin construct was forced to extend in water with pulling velocities of 0.005–0.05 nm/ps and with constant forces of 1000–2500 pN respectively. Resulting force-extension profiles exhibited a dual-peak pattern on various velocities, while both plateaus and shoulders appeared in the extension-time profiles on various forces. The force or extension profiles along stretching pathways were correlated to the conformational changes, suggesting that the structural collapses of P-selectin Lec/EGF domains were mainly attributed to the burst of hydrogen bonds within the major β sheet of EGF domain and the disruptions of two hydrophobic cores of Lec domain. This work furthers the understanding of forced dissociation of P-selectin/ligand bond.

Keywords: force, extension, P-selectin, steered molecular dynamics.

DOI: 10.1360/03ww0164

P-selectin, one of cellular adhesive molecules in selectin family, is a ~789 amino acid long chain. P-selectin/ligand interactions are important to many biological processes such as inflammatory cascade as well as tumor metastasis^[1,2]. During the inflammatory response, leukocytes expressing P-selectin ligand transiently roll over the surface of activated endothelial cells or platelets expressing P-selectin under blood flow. To balance the rear and front of the rolling cell and abate the impulsive force suffered by P-selectin/ligand bond, P-selectin and its ligand are stretched by applied shear force in certain content before the dissociation of P-selectin/ligand bond.

Forced dissociation of P-selectin/ligand bond has attracted the intensive interests of scientists upon the biological and biophysical significances. Atomic force microscope (AFM) and flow chamber assays were widely used to measure the rupture force and forced lifetime of P-selectin/PSGL-1 (P-selectin glycoprotein ligand-1) bond, attempting to understand the force dependence of bond

dissociation. While the nature that the bond lifetime is shortened by forces (so-called the slip bond^[3]) has been observed extensively^[4–6], the counter-intuitive nature that the bond lifetime is prolonged by forces (so-called the catch bond^[7]) was directly visualized recently^[8]. The underlying mechanism, however, of forced manipulation of P-selectin/ligand bonds has been little known. Explanation of the catch bond existence, for example, requires the further understanding of intra-molecular dynamics under applied forces while the experiment has not yet resolved the details of bond dissociation.

To conduct such a test, X-ray crystallography of protein and steered molecular dynamics (SMD) simulations were combined in this study to probe the forced stretching of P-selectin. P-selectin consists of an N-terminal, calcium-type lectin domain (Lec), an epidermal growth factor (EGF)-like domain, nine copies of consensus repeat units (CR1–9) characteristic of complement binding proteins, a transmembrane segment (TM), and a short cytoplasmic domain (Cyto)^[9], as illustrated in the upper panel of Fig. 1. Being the basic units which can mediate the leukocyte adhesion independently, human P-selectin Lec/EGF domains and its complex with PSGL-1 have been crystallized independently to obtain their X-ray structures^[10]. The overall folding of P-selectin Lec domain, analogous to other Ca^{2+} -dependent lectins^[10,11], consists of two α -helices, six β strands, and long loops or turns between two β strands or two α -helices. As conservative components of all C-type lectins, part of the second β strand (TRP⁵⁰-ILE⁵³) demarcates two distinct hydrophobic cores^[11]. While one core is composed of residues from the first β strand, the first α -helix, the part of inter-helix region, the part of second β strand and the sixth β strand, the other consists of residues from another part of inter-helix region, the second α helix to third β strand, the part of loops between the third and forth β strands, and other three β strands. The calcium ion is co-ordinated by the side chains of GLU⁸⁰, ASN⁸², ASN¹⁰⁵, ASP¹⁰⁶ and the backbone carbonyl of ASP¹⁰⁶. The binding “pocket”, composed of PRO⁴³-ILE⁵¹, TRP⁷⁶-LYS¹¹³ and calcium ion, forms the adhesive site of P-selectin/ligand interaction^[10]. P-selectin EGF domain, one member in EGF family, is partly defined by the strict conservation of six cysteines forming three disulfide bonds and two regions of double-stranded anti-parallel β sheet. While the major β sheet, close to the N-terminal subdomain (GLY¹³¹-CYS¹⁴⁴), contains two disulfide bonds (CYS¹²²-CYS¹³³, CYS¹²⁷-CYS¹⁴²), the minor β sheet, close to the C-terminal subdomain (PHE¹⁴⁸-VAL¹⁵⁶), contains the third disulfide bond (CYS¹⁴⁴-CYS¹⁵³)^[10,12]. Similar to the E-selectin Lec/EGF construct^[13], the two domains interact *via* a small interface.

Upon the advantage of molecular dynamics (MD) simulation which provides the time-dependent conformational changes in atomic level, SMD technique was

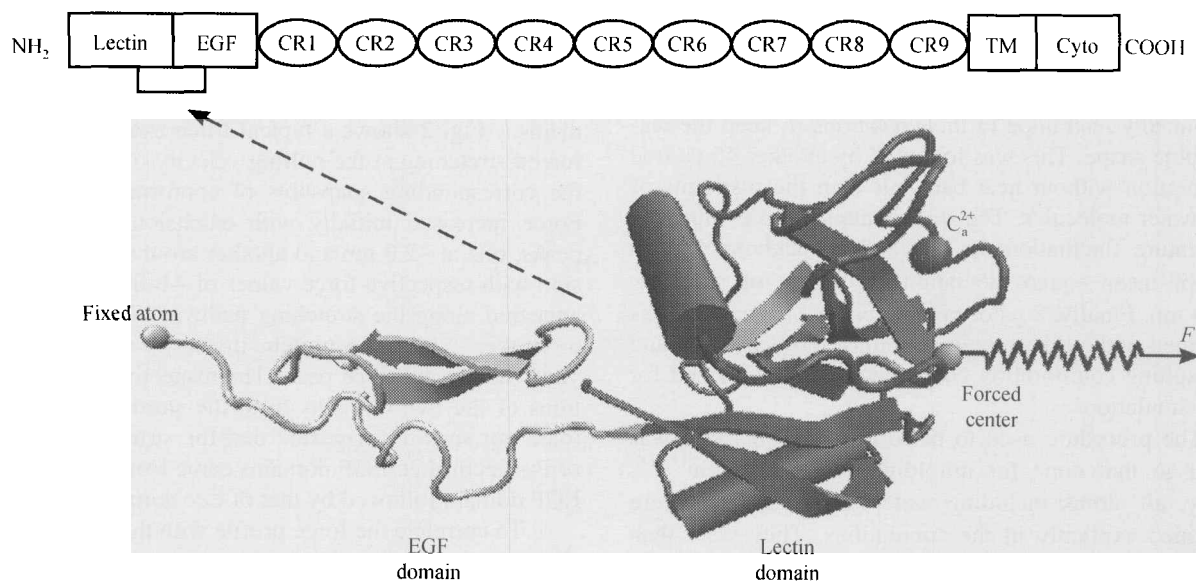


Fig. 1. Upper panel: Structure of P-selectin molecule; Lower panel, SMD simulations. Secondary structure of P-selectin Lec/EGF domains was exemplified with explicit position of calcium ion, and fixed atom, forced center, and applied force were illustrated.

recently developed by introducing external forces into molecular dynamics simulations with similar approaches in AFM assays^[14]. The applications of SMD have been focused on two main aspects. One was to get important structural information and structure-function relationship by applying external forces to molecules complex, e.g. the dissociation of biotin from avidin or streptavidin^[15,16], the unbinding of retinal from bacteriorhodopsin^[17], the release of phosphate from actin^[18], the possible binding pathways of thyroid hormone to its receptor, the extraction of lipids from membranes^[19,20], the unbinding of arachidonic acid from the prostaglandin H₂ synthase-1^[21], and forced detachment of the CD2-CD58 complex^[22]. The other was to investigate the elastic property by forced stretching or unfolding of biomolecules, e.g. the forced unfolding of titin immunoglobulin domains^[23], and the force-induced unfolding of titin fibronectin type III domains^[24].

To understand the role of P-selectin extension in forced dissociation of P-selectin/ligand interaction, P-selectin Lec/EGF domains were forced to extend under various constant velocities and constant forces using SMD simulations in this study. Corresponding force-extension profiles, extension-time profiles, as well as dynamic conformational changes were obtained, providing the new insights into forced stretching of P-selectin as well as dissociation of P-selectin/ligand bonds under physiological flow.

1 Methods

SMD simulations of forced stretching of P-selectin subunits were performed using the program NAMD2^[25] with the CHARMM22 force field^[26], plus the programs

XPLO^[27] and VMD^[28] for hydrogen bond analyses and structural visualizations respectively. The simulations started from an experimentally solved complex, using X-ray crystallography^[29], of P-selectin Lec/EGF domains binding to PSGL-1 peptide, deposited as entry 1G1S in the Protein Data Bank^[30].

Monomeric P-selectin Lec/EGF domains, the chain A adopted from the PDB 1G1S, were complemented with hydrogen atoms for all amino residues using PSFGEN^[25] procedure of NAMD2. A corresponding strontium ion (Sr²⁺) in the original structure was replaced by a calcium ion (Ca²⁺) since P-selectin/PSGL-1 binding is Ca²⁺-dependent in biological processes^[9]. The structure of P-selectin Lec/EGF domains was then solvated using the plug-in package SOLVATE 1.2^[28] of VMD with TIP3P model for explicit water molecules parameters^[31]. A sphere of radius of 4.5 nm was constructed, and all water molecules within 0.26 nm of the protein surface or within the volume occupied by the protein were deleted. The resulting initial configuration of P-selectin Lec/EGF domains, centered in the spherical water bubble, had the protein surface covered everywhere by at least 4–5 shells of water molecules (only the part of C-terminal of EGF domain has 2–3 water shells) with ~35750 atoms totally.

Before heating the water-protein system, the initial configuration was minimized for 3000 steps (2000 steps with fixed backbone atoms and then 1000 steps without any fixation) to modulate the conformational variation due to the adoption of monomeric P-selectin Lec/EGF domains from the complex, the substitution of Sr²⁺ with Ca²⁺, and the involvement of water molecules. Then the system was heated over 10 picosecond (ps) to 300 K with 30 K

ARTICLES

temperature increments per ps and in turn equilibrated with a thermal bath at 300 K for another 10 ps. During the equilibration process with thermal bath, water molecules composed of the outer 0.7 nm shell of the system were harmonically restrained to their positions to keep the water bubble shape. This was followed by another 45 ps free equilibration without heat bath but with the restraints of outer water molecules. The free dynamics run exhibited a temperature fluctuation of 4 K and a backbone RMSD (root of mean square deviation) evolution of (0.082 ± 0.007) nm. Finally, 2 ps of completely free dynamics was performed without harmonic restraints and heat bath, and the resulting equilibration conformation was obtained for SMD simulations.

The procedure used to perform the simulations was similar to that done for unfolding of titin protein^[23,24]. Briefly, all atoms including water and hydrogens were positioned explicitly in the simulations. They were then accomplished with a time step of 1 femtosecond (fs), a uniform dielectric constant of 1.0, a cut-off of non-bonded interactions with a switching function starting at a distance of 1.1 nm and reaching zero at 1.4 nm, and the scaling factor for 1-4 interactions of 1.0.

SMD simulations of forced stretching of P-selectin Lec/EGF domains were performed by fixing C-terminal of EGF domain and applying external forces to pulled end of Lec domain (seen in the lower panel of Fig. 1). Here C $_{\alpha}$ atom of ASP¹⁵⁸ was fixed, and the pulled end was defined as the mass center of eight atoms (N of SER⁴⁶, OG of SER⁴⁶, OG of SER⁴⁷, ND2 of ASN⁸², NH1 of ARG⁸⁵, OE2 of GLU⁸⁸, N of LYS¹¹², and NE2 of HSD¹¹⁴) within the binding pocket to PSGL-1^[10]. While the force direction was designated along the vector from the fixed point to pulled end, the forces were applied by using *cv*-SMD and *cf*-SMD algorithms respectively^[14], corresponding to the procedures performed for rupture force^[32] and forced lifetime^[8] measurements of P-selectin/ligand dissociation in AFM assays. The *cv*-SMD algorithm is equivalent to attaching one harmonic spring end to the pulled end of the protein and pulling another end of the spring with a constant velocity v in the desired direction, while the *cf*-SMD algorithm is equivalent to stretching the pulled end of the protein with a constant force F_0 . Time dependence of force in the *cv*-SMD algorithm follows the equation $F = k(vt - \Delta x)$, where Δx is the extension of the pulled end from its original position at time $t = 0$, and k is the spring constant. The value of k was given at 4000 pN/nm^[23,24], corresponding to the thermal fluctuation of the constrained pulled end to $\delta x = \sqrt{(k_B T / k)} \approx 0.032$ nm.

2 Results

Six SMD simulations were performed for forced stretching of P-selectin Lec/EGF domains, beginning with

an equilibrated folded structure and being stopped at the extension of $\Delta x \sim 8$ nm. Force and extension profiles were correlated with the conformational variations.

(i) Forced extension of P-selectin Lec/EGF domains. Fig. 2 shows a typical force-extension profile of forced stretching at the pulling velocity of 0.01 nm/ps and the corresponding snapshots of conformational changes. Force increased initially with extension, and two force peaks, one at ~ 2.0 nm and another around ~ 4.9 nm extension with respective force values of ~ 1400 and ~ 3500 pN, appeared along the stretching pathway. The force needed to further extend the protein increased continuously beyond the second force peak. The respective RMSD evolutions of the two domains from the starting conformation (data not shown) suggested that the structure disruptions of P-selectin Lec/EGF domains came from the collapse of EGF domain followed by that of Lec domain.

To correlate the force profile with the conformational changes, the structural variations were visualized as exemplified in Figs. 2(b)–(f). Initial snapshot ($\Delta x = 0$ nm) included six hydrogen bonds within the major β sheet of EGF domain, seven hydrogen bonds between Lec and EGF domains, and three hydrogen bonds between the part of inter-helix region and the sixth β strand of Lec domain (Regions ①, ② and ③ in Fig. 2(b)). Two hydrogen bonds, one between the second β strand and inter-helix region and the other between the second β strand and the sixth β strand, served as a part of interface of two hydrophobic cores of Lec domain, and two water molecules, near the intermediate entry to the hydrophobic cores and within 0.35 nm of the conservative part of the second β strand, formed water-bridge between LEU²⁶ and GLY⁵² (Regions ③ and ④ in Fig. 2(b)). Fig. 2(c) shows the conformational changes right after the first force peak ($\Delta x = 2.56$ nm), mainly corresponding to the break-ups of all hydrogen bonds between two strands of the major β sheet of EGF domain as well as the three hydrogen bond breakages between Lec and EGF domains. From that on, little variations of EGF domain were observed for further stretching. The last three snapshots (Figs. 2(d)–(f)) demonstrated the conformational changes of Lec domain just before ($\Delta x = 3.95$ nm), around ($\Delta x = 4.86$ nm) and after ($\Delta x = 5.31$ nm) the second force peak. While five of seven hydrogen bonds between the two domains and one hydrogen bond between the inter-helix region and the sixth β strand broke up before the second force peak (Fig. 2(d)), the two hydrogen bonds at the interface of two hydrophobic cores and the water-bridge between LEU²⁶ and GLY⁵² were broken and the water molecule near LEU²⁶ went into the interface around the peak. This resulted in re-formation of water-bridge again between VAL²⁷ and GLY⁵² as a replacement of hydrogen bond of HN⁵²-O²⁷ (Fig. 2(e)). And then the re-formed water-bridge broke up and more water molecules went into the gradually-disrupted hydro-

phobic cores for further stretching (Fig. 2(f)). These data suggested that the breakages of two hydrogen bonds at the hydrophobic cores interface and the re-formation of water-bridge played an important role in the late-phase stretching.

(ii) Dependence of constant velocities. To model

the rupture force measurements on various constant velocities in AFM assay, three *cv*-SMD simulations were performed at pulling velocities of 0.05, 0.01 and 0.005 nm/ps respectively. The corresponding force-extension profiles, as shown in Fig. 3(a), demonstrated similar features of stretching processes with small variations in force

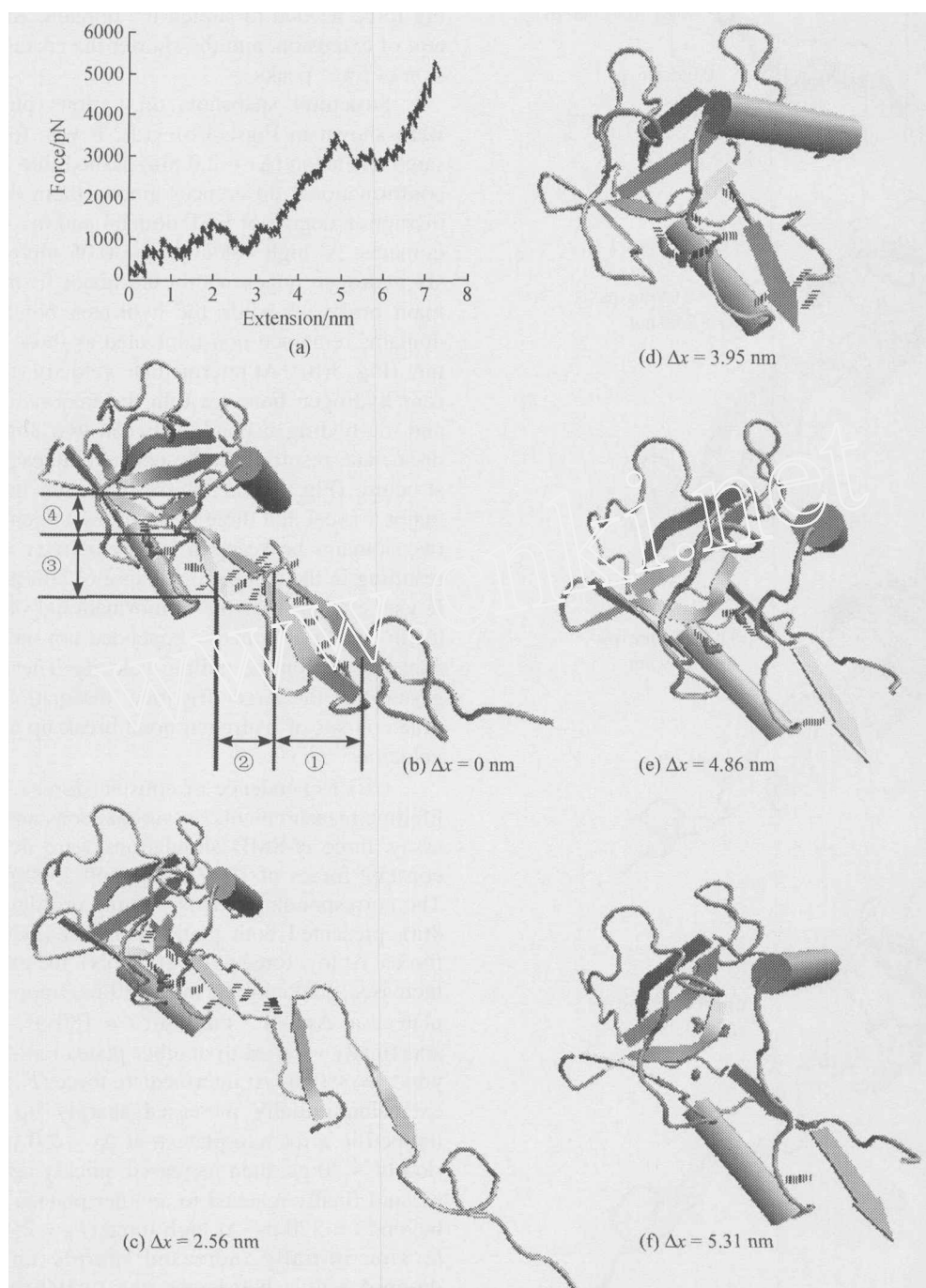


Fig. 2. Forced stretching of P-selectin Lec/EGF domains. (a) A typical force-extension profile at the pulling velocity of 0.01 nm/ps. (b) —(f) Structural snapshots of conformational changes on various extensions with explicit demonstrations of hydrogen bonds (parallel dashed lines) and water bridges (water molecules drawn as licorice model) distributions. Only Lec domain was shown up in (d)—(f) for clarity since little variations of EGF domain were found after the first force peak.

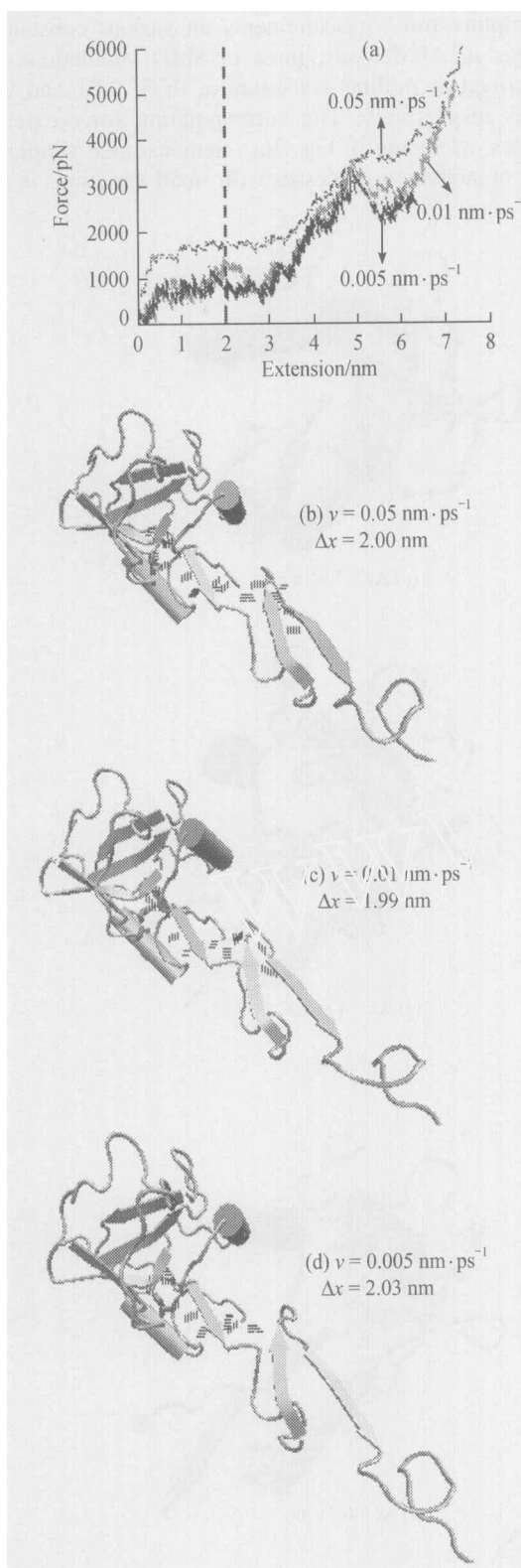


Fig. 3. Dependence of constant velocities on forced stretching of P-selectin Lec/EGF domains. (a) Force-extension profiles at various pulling velocities of 0.05, 0.01 and 0.005 nm/ps. (b)–(d) Corresponding snapshots at the extension of ~2.0 nm (dashed line) at three velocities.

peak values and corresponding extensions. At low pulling velocity ($v = 0.005$ nm/ps), the force profiles unveiled two force peaks, very similar to that as above at $v = 0.01$ nm/ps. At high velocity ($v = 0.05$ nm/ps), the first force peak became disappeared. These resulting profiles showed that the lower the pulling velocity, the smaller the corresponding force needed to stretch the domains to the same content of extension, and the shorter the corresponding extension of force peaks.

Structural snapshots on various pulling velocities were shown in Figs. 3(b)–(d). It was found that at the same extension ($\Delta x \sim 2.0$ nm; dashed line in Fig. 3(a)) the conformational differences among them depended on the disruption degree of EGF domain and the interface of two domains. At high velocity ($v = 0.05$ nm/ps), only two of six hydrogen bonds within the major β sheet of EGF domain broke up while the hydrogen bonds between two domains remained non-unraveled as those of initial structure (Fig. 3(b)). At intermediate velocity ($v = 0.01$ nm/ps), four hydrogen bonds within the major β sheet broke up and the hydrogen bonds between two domains started to dissociate, resulting in the partial collapse of anti-parallel structure (Fig. 3(c)). All six hydrogen bonds within the major β sheet and three of seven hydrogen bonds between two domains broke up at low velocity ($v = 0.005$ nm/ps), resulting in the complete collapse of anti-parallel structure. It was evident that the conformational changes of P-selectin Lec/EGF domains depended not only on the extension but also on the pulling velocity. These data also suggested that the larger frictional dissipation prolonged the time courses of hydrogen bond break-up at higher pulling velocities.

(iii) Dependence of constant forces. To mimic the lifetime measurements on various constant forces in AFM assay, three *cf*-SMD simulations were done by applying constant forces of 1000, 1500, and 2500 pN respectively. The corresponding extension-time profiles, shown in Fig. 4(a), presented both plateaus and shoulders on constant forces. At low force ($F_0 = 1000$ pN), the extension initially increased gradually up to $t = 80$ ps, trapped in a constant plateau at $\Delta x \sim 1.5$ nm until $t = 180$ ps, increased again and finally reached to another plateau at $\Delta x \sim 3.5$ nm beyond $t = 380$ ps. At intermediate force ($F_0 = 1500$ pN), the extension initially increased sharply up to $t = 35$ ps, trapped in a relative plateau at $\Delta x \sim 2.0$ nm for short period of ~ 20 ps, then increased quickly again until $t = 140$ ps, and finally reached to another plateau at $\Delta x \sim 3.8$ nm beyond $t = 220$ ps. At high force ($F_0 = 2500$ pN), the extension initially increased sharply up to $t = 50$ ps, dropped a little before entering a relatively variable plateau for a period of ~ 55 ps and then increased again from $t = 120$ ps.

Structural snapshots on various forces were shown in Figs. 4(b)–(d). It was found that at the same time ($t = 156$

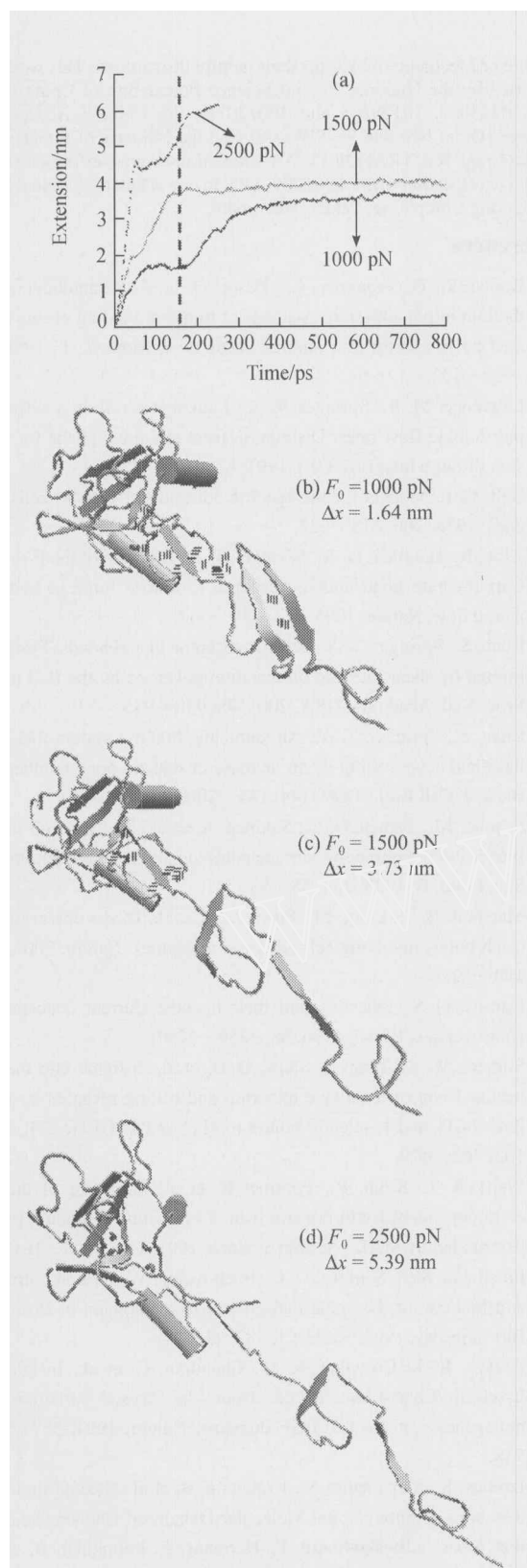


Fig. 4. Dependence of constant forces on forced stretching of P-selectin Lec/EGF domains. (a) Extension-time profiles at various applied forces of 2500, 1500, and 1000 pN. (b)–(d) Corresponding snapshots at the stretching time of 156 ps (dashed line) at three applied forces.

ps; dashed line in Fig. 4(a)) the corresponding extensions differed significantly from each other ($\Delta x \sim 1.64$ – 5.39 nm). At low force ($F_0 = 1000$ pN and $\Delta x = 1.64$ nm), the structural conformation of P-selectin Lec/EGF domains was the same as the initial one except that four of six hydrogen bonds within the major β sheet of EGF domain broke up (Fig. 4(b)). At intermediate force ($F_0 = 1500$ pN and $\Delta x = 3.73$ nm), the EGF domain collapsed completely accompanied with partial unraveling of two hydrophobic cores (Fig. 4(c)). At high force ($F_0 = 2500$ pN and $\Delta x = 5.39$ nm), both P-selectin Lec and EGF domains collapsed completely, the interface of two hydrophobic cores became disappeared, and the cores opened their doors to let more water molecules enter into.

3 Discussion

The aim of this study is to elucidate, on the basis of atom-level simulations, the conformational changes of forced stretching of P-selectin Lec/EGF domains. On applied constant velocities, SMD simulations found that there existed two peaks in the force-extension profiles, which were correlated with the structural collapse of EGF domain at ~ 2.0 nm followed by that of Lec domain at ~ 4.9 nm (Figs. 2 and 3). This dual-peak force pattern differed significantly from the simulations in unfolding of titin Ig domains^[23], while the latter unveiled one force peak within $\Delta x \sim 8$ nm. Current simulations implied two major energy barriers suffered along the extension pathway: the outer one is based on intrinsic hydrogen bond interactions within the major β sheet of EGF domain and the inner one resulted from the re-formation of water bridge between GLY⁵² and VAL²⁷ after the breakage of two hydrogen bonds (HN⁵²-O²⁷ and HN⁵⁰-O¹¹⁴) at the interface of two hydrophobic cores of Lec domain. At the highest pulling velocity of $v = 0.05$ nm/ps, forces were large enough that the outer barrier was eliminated. On applied constant forces, SMD simulations revealed the shoulders and plateaus pattern (Fig. 4), similar to that found in the extension-time profiles of dissociation of CD2-CD58 complex at a low force $F_0 = 400$ pN^[22]. These simulations suggested that the P-selectin Lec/EGF domains became trapped in the plateaus on its pathway to be extensively stretched, and the plateaus corresponded to the energy barriers where conformations of P-selectin Lec/EGF domains changed little. At the highest force ($F_0 = 2500$ pN), force was large enough that the first plateau shown in the extension-time profiles at $F_0 = 1000$ and 1500 pN became disappeared. The above observations were confirmed in the additional SMD simulations using lightly varied force centers and directions or using different initial equilibrated conformations (data not shown). Combined together, these simulations demonstrated similar features of energy barriers on both constant velocity-induced and constant force-

ARTICLES

induced extensions.

Under physiological flow, transient rolling of leukocytes over the activated endothelial cells and/or platelets come from the balance of dissociation of a selectin/ligand bond in the rear of a rolling cell to formation of another bond in the front of the cell; otherwise leukocytes would detach back to the main stream if no bonds form in the front when bonds in the rear break up, or would form the confirmed adhesion if more bonds form in the front when no bonds break up in the rear. To hold the consecutive rolling, selectin molecule in the rear is required physiologically to extend before it dissociates from its ligand under shear flow. Not only such a phenomena has been observed experimentally by the flow chamber assay^[1,2,4,6], but it was also demonstrated by our preliminary SMD simulations in unbinding of P-selectin/PSGL-1 complex. In fact, the anti-parallel β sheet in EGF domain collapsed before the PSGL-1 dissociated from P-selectin molecule (data not shown), which is similar to the SMD simulations shown in unbinding of CD2/CD58 complex^[22].

Main shortcomings of SMD simulations are the short simulation times and the small size of system imposed by the limited computer resources when one attempts to compare the simulations with the measurements using AFM assay. Five- to six-order of higher velocities (*cv*-SMD) or two-order of higher forces (*cf*-SMD) and two-order of higher spring constants were used in SMD simulations than those in AFM measurements, which resulted in the non-equilibrium process with strong energy dissipation. As such, large fraction of work done by applied forces was used to overcome the frictional dissipation rather than to lower energy barrier(s). In our simulations, the system temperature increased by 3—4 and 5—6 K at $v = 0.01$ and 0.05 nm/ps, respectively, up to $\Delta x \sim 8$ nm. To repair this deficit, improved computer resources are needed with which SMD simulations with several tens of nanoseconds and several hundred thousands of atoms may become available soon. And improved algorithms in the simulations enable to save the computational expense upon the same resources.

Even with the shortcomings mentioned above, SMD simulations in the present investigation were still demonstrated as a powerful tool in forced stretching of protein molecules. Using a limited computational expense, key features of conformational variations of P-selectin Lec/EGF domains were obtained on applied forces. A recently completed P-selectin/PSGL-1 unbinding experiment^[18] showed a counter-intuitive nature of catch bond; SMD simulations to reveal the dissociation process of P-selectin/PSGL-1 complex is ongoing.

Acknowledgements The authors are grateful to Drs. Jizhong Lou and Cheng Zhu in Georgia Institute of Technology, USA, and Dr. Bo Huo in

Institute of Mechanics, CAS, for their helpful discussions. This work was supported by the National Natural Science Foundation of China (Grant Nos. 30225027, 10128205 and 10072071), the Chinese Academy of Sciences (Grant No. KJCX2-SW-L06), and the Ministry of Education of China (Grant No. TRAPOYT). All simulations were performed on the parallel workstation IBM RS/6000 SP3 in the Center of Science and Engineering Computing, Peking University.

References

1. Kaplanski, G., Franarier, C., Tissot, O. et al., Granulocyte-endothelium initial adhesion: Analysis of transient binding events mediated by E-selectin in a laminar shear flow, *Biophys. J.*, 1993, 64: 1922—1933.
2. Lawrence, M. B., Springer, T. A., Leukocytes roll on a selectin at physiologic flow rates: Distinction from and prerequisite for adhesion through integrins, *Cell*, 1991, 65: 859—873.
3. Bell, G. I., Models for the specific adhesion of cells to cells, *Science*, 1978, 200: 618—627.
4. Alon, R., Hammer, D. A., Springer, T. A., Lifetime of the P-selectin: Carbohydrate bond and its response to tensile force in hydrodynamic flow, *Nature*, 1995, 374: 539—542.
5. Chen, S., Springer, T. A., Selectin receptor-ligand bonds: Formation limited by shear rate and dissociation governed by the Bell model, *Proc. Natl. Acad. Sci. USA*, 2001, 98: 950—955.
6. Chen, S., Springer, T. A., An automatic braking system that stabilizes leukocyte rolling by an increase in selectin bond number with shear, *J. Cell Biol.*, 1999, 144: 185—200.
7. Dembo, M., Torney, D. C., Saxman, K. et al., The reaction-limited kinetics of membrane-to-surface adhesion and detachment, *Proc. R. Soc. Lond. B*, 1988, 234: 55—83.
8. Marshall, B. T., Long, M., Piper, J. W. et al., Direct observation of catch bonds involving cell-adhesion molecules, *Nature*, 2003, 423: 190—193.
9. Kansas, G. S., Selectins and their ligands: Current concepts and controversies, *Blood*, 1996, 88: 3259—3287.
10. Somers, W. S., Tang, J., Shaw, G. D. et al., Insights into the molecular basis of leukocyte tethering and rolling revealed by structures of P- and E-selectin bound to sLe^x and PSGL-1, *Cell*, 2000, 103: 467—479.
11. Weis, W. I., Kahn, R., Fourme, R. et al., Structure of the calcium-dependent lectin domain from a rat mannose-binding protein determined by MAD phasing, *Science*, 1991, 254: 1608—1615.
12. Freedman, S. J., Sanford, D. G., Bachovchin, W. W. et al., Structure and function of the epidermal growth factor domain of P-selectin, *Biochemistry*, 1996, 35(43): 13733—13744.
13. Graves, B. J., Crowther, R. L., Chandran, C. et al., Insight into E-selectin/Ligand interaction from the crystal structure and mutagenesis of the Lec/EGF domains, *Nature*, 1994, 367: 532—538.
14. Izrailev, S., Stepaniants, S., Israilewitz, B. et al., Steered molecular dynamics, *Computational Molecular Dynamics: Challenges, Methods, Ideas* (eds. Deuffhard, P., Hermans, J., Leimkuler, B. et al.), Berlin: Springer-Verlag, 1998, 4: 39—65.
15. Izrailev, S., Stepaniants, S., Balsera, M. et al., Molecular dynamics study of unbinding of the avidin-biotin complex, *Biophys. J.*, 1997, 72: 1568—1581.

16. Grubmüller, H., Heymann B., Tavan P., Ligand binding: Molecular mechanics calculation of the streptavidin-biotin rupture force, *Science*, 1996, 271: 997—999.
17. Isralewitz, B., Izrailev, S., Schulten, K., Binding pathway of retinal to bacterio-opsin: A prediction by molecular dynamics simulations, *Biophys. J.*, 1997, 73: 2972—2979.
18. Wriggers, W., Schulten, K., Investigating a back door mechanism of actin phosphate release by steered molecular dynamics, *Proteins: Struct. Func. & Genetics*, 1999, 35: 262—273.
19. Stepaniants, S., Izrailev, S., Schulten, K., Extraction of lipids from phospholipid membranes by steered molecular dynamics, *J. Mol. Model*, 1997, 3: 473—475.
20. Marrink, S.-J., Berger, O., Tieleman, P. et al., Adhesion forces of lipids in a phospholipid membrane studied by molecular dynamics simulations, *Biophys. J.*, 1998, 74: 931—943.
21. Molnar, F., Norris, L. S., Schulten, K., Simulated unbinding and binding of fatty acid substrates in the cyclooxygenase site of prostaglandin H₂ synthase-1, *Progress in Reaction Kinetics and Mechanism*, 2000, 25: 263—298.
22. Bayas, M. V., Schulten, K., Leckband, D., Forced detachment of the CD2-CD58 complex, *Biophys. J.*, 2003, 84: 2223—2233.
23. Lu, H., Isralewitz, B., Karmmer, A. et al., Unfolding of titin Immunoglobulin domains by steered molecular dynamics simulation, *Biophys. J.*, 1998, 75: 662—671.
24. Gao, M., Craig, D., Vogel, V. et al., Identifying unfolding intermediates of FN-III₁₀ by steered molecular dynamics, *J. Mol. Biol.*, 2002, 323: 939—950.
25. Kalé, L., Skeel, R., Bhandarkar, M. et al., NAMD2: greater scalability for parallel molecular dynamics, *J. Comput. Phys.*, 1999, 151: 283—312.
26. Mackerell, A. D. Jr., Bashford, D., Bellot, M. et al., All-atom empirical potential for molecular modeling and dynamics studies of proteins, *J. Phys. Chem. B*, 1998, 102: 3586—3616.
27. Brünger, A. T., *X-PLOR*, Version 3.1: A System for X-ray Crystallography and NMR, New Haven, CT: The Howard Hughes Medical Institute and Department of Molecular Biophysics and Biochemistry, Yale University, 1992.
28. Humphrey, W., Dalke, A., Schulten, K., VMD: Visual molecular dynamics, *J. Mol. Graph.*, 1996, 14: 33—38.
29. Stout, G. H., Jensen, L. H., *X-ray Structure Determination: A Practical Guide*, New York: John Wiley & Sons Inc, 1989.
30. Bernstein, F. C., Koetzle, T. F., Williams, G. J. B. et al., The protein data bank: A computer-based archival file for macromolecular structures, *J. Mol. Biol.*, 1977, 112: 535—542.
31. Jorgensen, W. L., Chandrasekhar, J., Madura, J. D., Comparison of simple potential functions for simulating liquid water, *J. Chem. Phys.*, 1983, 79: 926—935.
32. Fritz, J., Katopodis, A. G., Kolbinger, F. et al., Force-mediated kinetics of single P-selectin/ligand complexes observed by atomic force microscopy, *Proc. Natl. Acad. Sci. USA*, 1998, 95: 12283—12288.

(Received September 16, 2003; accepted October 22, 2003)

Chinese Science Bulletin 2004 Vol. 49 No. 1 17—22

Linearly programmed DNA-based molecular computer operated on magnetic particle surface in test-tube

ZHAO Jian*, ZHANG Zhizhou*, SHI Yongyong, Li Xiuxia & HE Lin

Bio-X Life Science Research Center, Shanghai Jiao Tong University, Shanghai 200030, China

* The authors did equal contributions to the work.

Correspondence should be addressed to He Lin or Zhang Zhizhou (e-mail: helin@sjtu.edu.cn or zhangzz@sjtu.edu.cn)

Abstract The postgenomic era has seen an emergence of new applications of DNA manipulation technologies, including DNA-based molecular computing. Surface DNA computing has already been reported in a number of studies that, however, all employ different mechanisms other than automaton functions. Here we describe a programmable DNA surface-computing device as a Turing machine-like finite automaton. The laboratory automaton is primarily composed of DNA (inputs, output-detectors, transition molecules as software), DNA manipulating enzymes and buffer system that solve artificial computational problems autonomously. When fluoresceins were labeled in the 5' end of (–) strand of the input molecule, direct observation of all reaction intermediates along the time scale was made so that the dynamic process of DNA computing could be conveniently visualized. The features of this study are: (i) achievement of finite automaton functions by linearly programmed DNA computer operated on magnetic particle surface and (ii) direct detection of all DNA computing intermediates by capillary electrophoresis. Since DNA computing has the massive parallelism and feasibility for automation, this achievement sets a basis for large-scale implications of DNA computing for functional genomics in the near future.

Keywords: DNA, computing, automaton, surface, parallelism, programmable.

DOI: 10.1360/03wc0357

Researchers across multi-disciplines in the world are making great efforts in the revolution of traditional computers by endeavor in DNA-based computing. The first small-scale molecular computation with DNA was brilliantly demonstrated by Adleman^[1], and seven years after that, Shapiro and co-workers reported their programmable and autonomous test-tube computing machine made of biomolecules^[2]. This computing machine is actually a finite automaton capable of state transitions, marking the milestone of the birth of DNA computer. Before Shapiro's pioneering work, there were a number of reports on DNA computing successful for solving NP problems^[3–6]. Given that the input data for DNA computing are within DNA